




**ORIGINAL ARTICLE**

# Hydrogen-deuterium exchange mass spectrometry highlights conformational changes induced by factor XI activation and binding of factor IX to factor XIa

Awital Bar Barroeta<sup>1</sup>  | Josse van Galen<sup>1</sup> | Ingrid Stroo<sup>1</sup> | J. Arnoud Marquart<sup>1</sup> | Alexander B. Meijer<sup>1,2</sup>  | Joost C. M. Meijers<sup>1,3</sup> 

<sup>1</sup>Department of Molecular and Cellular Hemostasis, Sanquin Research, Amsterdam, The Netherlands

<sup>2</sup>Department of Pharmaceutics, Utrecht Institute for Pharmaceutical Sciences (UIPS), Utrecht University, Utrecht, The Netherlands

<sup>3</sup>Department of Experimental Vascular Medicine, Amsterdam UMC, University of Amsterdam, Amsterdam, The Netherlands

**Correspondence**

Joost C. M. Meijers, Department of Molecular and Cellular Hemostasis, Sanquin Research, Plesmanlaan 125, 1066 CX Amsterdam, The Netherlands.  
Email: j.meijers@sanquin.nl

**Funding information**

Landsteiner Foundation for Blood Transfusion Research, Grant/Award Number: 1702; Ministerie van Volksgezondheid, Welzijn en Sport, Grant/Award Number: PPOP-14-01

**Abstract**

**Background:** Factor XI (FXI) is a zymogen in the coagulation pathway that, once activated, promotes haemostasis by activating factor IX (FIX). Substitution studies using apple domains of the homologous protein prekallikrein have identified that FIX binds to the apple 3 domain of FXI. However, the molecular changes upon activation of FXI or binding of FIX to FXIa have remained largely unresolved.

**Objectives:** This study aimed to gain more insight in the FXI activation mechanism by identifying the molecular differences between FXI and FXIa, and in the conformational changes in FXIa induced by binding of FIX.

**Methods:** Hydrogen-deuterium exchange mass spectrometry was performed on FXI, FXIa, and FXIa in complex with FIX.

**Results:** Both activation and binding to FIX induced conformational changes at the interface between the catalytic domain and the apple domains of FXI(a)—more specifically at the loops connecting the apple domains. Moreover, introduction of FIX uniquely induced a reduction of deuterium uptake in the beginning of the apple 3 domain.

**Conclusions:** We propose that the conformational changes of the catalytic domain upon activation increase the accessibility to the apple 3 domain to enable FIX binding. Moreover, our HDX MS results support the location of the proposed FIX binding site at the beginning of the apple 3 domain and suggest a mediating role in FIX binding for both loops adjacent to the apple 3 domain.

**KEYWORDS**

factor IX, factor XI, factor XIa, hemostasis, mass spectrometry

Manuscript handled by: James Morrissey

Final decision: James Morrissey, 19 August 2019

This is an open access article under the terms of the Creative Commons Attribution-NonCommercial-NoDerivs License, which permits use and distribution in any medium, provided the original work is properly cited, the use is non-commercial and no modifications or adaptations are made.

© 2019 The Authors. *Journal of Thrombosis and Haemostasis* published by Wiley Periodicals, Inc. on behalf of International Society on Thrombosis and Haemostasis

## 1 | INTRODUCTION

Factor XI (FXI) is the zymogen of coagulation protease factor XIa (FXIa), a 160 kDa dimer with a supportive role in haemostasis.<sup>1-4</sup> FXIa promotes thrombin generation by activating factor IX (FIX). FXI(a) function is related to propagation of fibrin clot formation and protecting the fibrin clot from degradation.<sup>3,4</sup> Accordingly, FXI deficiency is associated with mild bleeding disorders.<sup>5</sup> Nevertheless, FXI seems to play a role in thrombosis as increased levels of FXI have been linked to higher risks of both venous and arterial thromboembolism.<sup>4,6-9</sup>

The FXI monomers are made up of two distinct chains: a light and a heavy chain.<sup>10</sup> The light chain consists of a catalytic domain, whereas the heavy chain contains four apple domains. Each apple domain has seven antiparallel  $\beta$ -strands that form a sheet supporting a single  $\alpha$ -helix. Moreover, the four apple domains form a disc-like base for the catalytic domain, which resembles a saucer under a cup.<sup>10</sup> Each monomer can be activated through cleavage of the Arg<sup>369</sup>-Ile<sup>370</sup> bond by either thrombin or factor XIIa.<sup>1,10,11</sup> Cleavage releases an activation loop that inserts itself into the activation pocket of FXIa, which is characteristic for serine proteases.<sup>10</sup> This movement can be observed as a 20 Å shift of Ile<sup>370</sup> in the crystal structure of the catalytic domain of FXIa compared to the structure of FXI.<sup>10,12</sup>

Additionally, FXI activation induces structural changes that enable FIX binding, since FIX can bind FXIa but not FXI.<sup>13,14</sup> FXI has been shown to accommodate the FIX Gla domain at an exosite in the apple 3 domain, including amino acids Ile<sup>183</sup>, Arg<sup>184</sup>, and Asp<sup>185</sup>.<sup>15</sup> Since it is buried in the FXI zymogen, the structural changes that allow FIX binding are thought to reveal the exosite.<sup>13,15-18</sup> However, the full crystal structure of FXIa is yet to become available to confirm this.

FXI is a close homologue of prekallikrein.<sup>16,19,20</sup> The crystal structure of kallikrein was recently elucidated and its structure was compared to a model of prekallikrein.<sup>20</sup> In this study a major change in surface exposure was proposed for the loop connecting the apple 3 and apple 4 domains. The loop is buried in the prekallikrein model and becomes exposed in kallikrein, increasing the accessibility of the apple 3 domain surface.<sup>20</sup> Moreover, a 180° horizontal shift in the orientation of the catalytic domain with respect to the heavy chain was observed.<sup>20</sup> This was accompanied by a change in the interactions of two latch loops, which extend from the catalytic domain and retain its interaction with the apple domains after the cleavage of the activation loop.<sup>20</sup>

This study aimed to investigate the structural changes that occur in FXI upon activation, thereby utilising the recently published crystal structure of kallikrein.<sup>20</sup> Furthermore, the structural changes induced by binding of FIX to FXIa were studied. Towards these goals, we performed hydrogen-deuterium mass spectrometry (HDX MS) on FXI, FXIa, and FXIa in complex with FIX to characterise the areas that undergo molecular changes either upon activation or by binding to FIX. HDX MS measures the extent of deuterium exchange of amide hydrogens in the protein backbone.

### Essentials

- Conformational changes in factor XI upon activation or binding of factor IX are largely unresolved.
- HDX mass spectrometry was performed with factor XI, factor XIa and factor XIa in complex with factor IX.
- The apple 3 domain and the loops between the apple domains change conformation upon factor XI activation.
- These conformational changes expose the binding site for factor IX and allow binding to the apple 3 domain.

This exchange depends on the flexibility and solvent accessibility of a protein domain.<sup>21</sup> Thus, differences in deuterium uptake can be assigned to a change in local structure or an altered interaction of a protein domain. Both activation of FXI and binding of FIX to FXIa seem to cause rigidification of the FXI(a) structure. Activation of FXI mainly induces molecular changes at the interface between the catalytic domain and the apple domains. Binding of FIX to FXIa mainly affects the beginning of the apple 3 domain and the loops flanking the apple 3 domain.

## 2 | MATERIALS AND METHODS

### 2.1 | Materials

QuikChange was from Agilent. HEK293 cells were from ATCC. Cell culture media used were DMEM/F12 (Lonza) and Opti-MEM I reduced serum medium with Glutamax supplement (Gibco; Thermo Fisher Scientific). Cell Factories and TripleFlasks were obtained from Thermo Fisher Scientific. Geneticin (G-418 Sulfate) was from Calbiochem (Merck). Peptide-IV (H-SDDDDWIPDIQTDPNGLSFNPNISDFPDTTSPK-OH)<sup>22</sup> was provided by Thermo Fisher Scientific and coupled to CNBr-Activated Sepharose 4 Fast Flow (GE Healthcare Life Sciences). A Fresenius Polysulfone low-flux dialyser F5HPS (Fresenius Medical Care, Bad Homburg von der Höhe, Germany) was used as an artificial kidney. Diisopropyl fluorophosphate (DFP) and polyethylene glycol (PEG) 6000 were purchased from Sigma-Aldrich. FIX was a kind gift from the late Dr. Walter Kiesel (Albuquerque, NM, USA). All materials for MS were obtained from Thermo Fisher Scientific, unless mentioned otherwise. For SDS-PAGE NuPAGE Novex 4-12% Bis-Tris protein gels and Imperial protein stain were used (Thermo Fisher Scientific).

### 2.2 | Cell culture, protein expression and protein purification

FXI-WT cDNA with Cys<sup>11</sup> replaced by Ser was introduced in pCDNA3.1.<sup>23</sup> FXI-S557A was prepared from FXI wild type (WT) by Quikchange mutagenesis. Sequence analysis was used to confirm the introduced mutation. FXI-WT and FXI-S557A were stably

transfected in HEK293 cells using calcium precipitation. Medium with 5% FCS was used to expand and grow cells in a Cell Factory (6320 cm<sup>2</sup>) for expression. At confluence, serum-free medium (Optimem/Glutamax 1) was added and collected every 48-72 hours. FXI was purified from expression medium using a peptide IV column<sup>23</sup> after concentrating the collected medium over an artificial kidney. The peptide IV column was eluted with 100 mmol/L citrate pH 5.0, 1 mol/L NaCl, and 10 mmol/L EDTA. The eluent was checked for contamination with FXIa with chromogenic substrate S2366. Contaminating enzymes, including FXIa, were eliminated by treatment with serine protease inhibitor DFP until chromogenic activity was inhibited. Purified protein was dialysed against 10 mmol/L HEPES, pH 7.5, containing 0.5 mol/L NaCl and stored at -80°C. The concentration of recombinant protein was determined by measuring the absorbance at 280 nm using the extinction coefficient for FXI (13.4).

### 2.3 | Activation of FXI to FXIa

FXI-WT or S557A was incubated with FXIIa (molar ratio 20:1) in assay buffer (25 mmol/L HEPES, 127 mmol/L NaCl, 3.5 mmol/L KCl, 3 mmol/L CaCl<sub>2</sub>) with 0.1% PEG6000 for 72 hrs at 37°C. FXIa or FXIa-S557A was purified using the peptide IV column as described above.

### 2.4 | Hydrogen-deuterium exchange mass spectrometry (HDX MS)

Protein samples (2 μmol/L FXI(a) or 2 μmol/L FXIa with 5 μmol/L FIX) were placed in a LEAP PAL pipetting robot (LEAP Technologies, Morrisville, NC, USA). Samples were diluted 10 times in binding buffer (10 mmol/L Hepes pH 7.4, 111 mmol/L NaCl, and 7 mmol/L CaCl<sub>2</sub> in 98% D<sub>2</sub>O), resulting in a final buffer composition of 10 mmol/L Hepes pH 7.4, 150 mmol/L NaCl and 7 mmol/L CaCl<sub>2</sub>, and samples were incubated for 10 seconds, 100 seconds or 1000 seconds at 24 °C. Incubation with binding buffer containing H<sub>2</sub>O instead of D<sub>2</sub>O was used as reference. Deuterium exchange was quenched by mixing the sample 1:1 with quenching solution (1 g TCEP dissolved in 2 mL 2 mol/L Urea, 1 mol/L NaOH) for 1 minute at 4°C. The sample was digested by passing it over a Poroszyme Immobilized Pepsin Cartridge with an isocratic flow of 5% acetonitrile, 0.1% formic acid for 5 minutes at 4°C. After collection on a trap (Acclaim Guard Column. 120, C18, 5 μm, 2.0 × 10 mm), the peptides were washed for 30 seconds at 4°C. Subsequently, peptides were eluted and passed over an analytic C18 column (Hypersil Gold C18) using a gradient from 4-64% acetonitrile at 50 μL/min at 4°C. Peptides were injected online into an LTQ Orbitrap-XL operating in positive mode. In order to identify peptides and their retention times, peptides were fragmented by collision induced dissociation, and the resulting data were analysed using PEAKS software (PEAKS 7.0; Bioinformatics Solutions Inc.). Deuterium uptake of the samples was calculated using HDExaminer 2.2.0 (Sierra Analytics). At least three independent experiments were performed to collect the data.

### 2.5 | HDX data analysis

The percentage deuterium uptake (%D) for all peptides generated with pepsin digestion was calculated with respect to peptide size and maximal amount of deuterium incorporation. This was analysed for FXI-WT, FXIa-WT, FXI-S557A, FXIa-S557A, and FXIa-S557 with FIX. Peptides that were not detected for FXI-WT or FXIa-WT were not considered in further analysis of FXI-S557A and FXIa-S557A (with FIX), respectively. Per detected peptide the average deuterium uptake (%) and standard deviation were calculated individually for each incubation time (10 seconds, 100 seconds or 1000 seconds). The reliability of the measurements was assessed per time point. If for a time point deuterium uptake in a peptide could not be measured in at least half of the measurements this data point was considered unreliable and excluded from the results. Furthermore, data points with a standard deviation greater than 5% were not included. The difference in deuterium uptake was calculated between FXIa-S557A and FXI-S557A as well as between FXIa-S557A with FIX and FXIa-S557A. Peptides were only included if they were measured in both compared samples. Furthermore, differences were deemed significant if these were consistently greater than 4%. The results were visualised in a 3D protein model using PyMol (Schrödinger).

### 2.6 | Construction of homology model

A homology model of FXIa based on kallikrein was constructed using MODELLER9.21. The amino acid sequences of FXI and kallikrein were aligned to ensure optimal overlap. Hereafter, five homology models were generated based on coordinates from kallikrein (PDB ID 6I44).<sup>20</sup> The homology model with the lowest DOPE score was chosen as a representative of the FXIa structure. Figures were generated using PyMOL (Schrödinger).

## 3 | RESULTS

### 3.1 | HDX MS of FXI, FXIa, and FXIa in complex with FIX

A catalytically inactive FXI mutant (S557A) was used to prevent auto-activation of FXI as well as the cleavage of FIX and subsequent release of FIXa. To assess whether this mutation influenced deuterium uptake of the protein, the deuterium uptake spectrum of the mutant in the zymogen or activated state was compared to that of the wild type proteins. The mutation did not influence the deuterium uptake for either FXI or FXIa (Figures S1 and S2), which allowed the use of the mutants for further experiments.

HDX MS was performed on FXI-S557A, FXIa-S557A, and FXIa-S557A in complex with FIX to identify protein regions that undergo molecular changes upon activation of FXI or binding of FIX to FXIa. For the HDX MS analysis changes in the percentage of deuterium uptake (%D) were calculated and plotted against the incubation times for each detected peptide (Figure 1). Figure 2 shows four examples of the trends that were observed for deuterium uptake in the complete

peptide set. For region Leu<sup>149</sup>-Leu<sup>163</sup> (Figure 2A, peptide 39) no difference in deuterium uptake was observed between FXI-S557A, FXIa-S557A, and FXIa-S557A with FIX. This suggests that the amino acids in this region have a similar conformation in the three protein states. Deuterium uptake in Ala<sup>181</sup>-Phe<sup>192</sup> (Figure 2B, peptide 52) shows no difference between FXIa and FXI, but is reduced in FXIa with FIX. Thus, this region is not influenced by FXI activation, but becomes more rigid or shielded by binding to FIX. A slight reduction in deuterium uptake is seen in FXIa for Phe<sup>260</sup>-Cys<sup>273</sup> (Figure 2C, peptide 74), which is more pronounced in FXIa with FIX, implying that the molecular change induced by activation is strengthened by FIX binding. Lastly, region Tyr<sup>503</sup>-Glu<sup>525</sup> (Figure 2D, peptide 128) shows the same reduction in deuterium uptake for FXIa and FXIa with FIX compared to FXI and is therefore only affected by activation. The deuterium uptake plots of the complete set of peptides detected in FXI, FXIa, and FXIa with FIX are included in Figures S3-S9.

### 3.2 | Activation of FXI increases accessibility to apple 3 domain

The amino acids shared by overlapping peptides with an altered deuterium uptake corresponding to activation were used to define

regions that vary between FXI and FXIa. These regions were highlighted in the crystal structure of FXI (Figure 3A, left). Consistent small reductions in deuterium uptake were observed for the loop connecting apple 2 and apple 3 (Ser<sup>171</sup>-Leu<sup>177</sup>, blue), one beta-strand in the apple 3 domain (Pro<sup>247</sup>-Gly<sup>259</sup>, orange), and the loop connecting apple 3 and apple 4 (Ser<sup>261</sup>-Phe<sup>272</sup>, dark orange). Furthermore, two regions that showed a reduced deuterium uptake upon activation were identified within the catalytic domain: Lys<sup>509</sup>-Glu<sup>525</sup> (cyan) and Cys<sup>581</sup>-Tyr<sup>590</sup> (yellow). Moreover, a clear reduction in deuterium exchange was observed for the loops between apple 1 and apple 2 (Tyr<sup>80</sup>-Ala<sup>91</sup>, pink).

These regions were then projected in a homology model of FXIa (Figure 3A, right) based on the recently published crystal structure of kallikrein (PDB ID 6I44)<sup>20</sup> and compared to their structure in FXI. A large reduction in accessibility was seen in the FXIa model for region Tyr<sup>80</sup>-Ala<sup>91</sup> (pink) as a result of a 180° turn of the catalytic domain (visible in the top view, Figure 3B) upon activation. In contrast, the large conformational change of the catalytic domain increased the accessibility of loop Ser<sup>171</sup>-Leu<sup>177</sup> (blue) and loop Phe<sup>260</sup>-Phe<sup>272</sup> (dark orange) after activation. This was most pronounced for the Phe<sup>260</sup>-Phe<sup>272</sup> region. Interestingly, the HDX MS results suggest either a decrease in accessibility or an increase in the rigidity of these

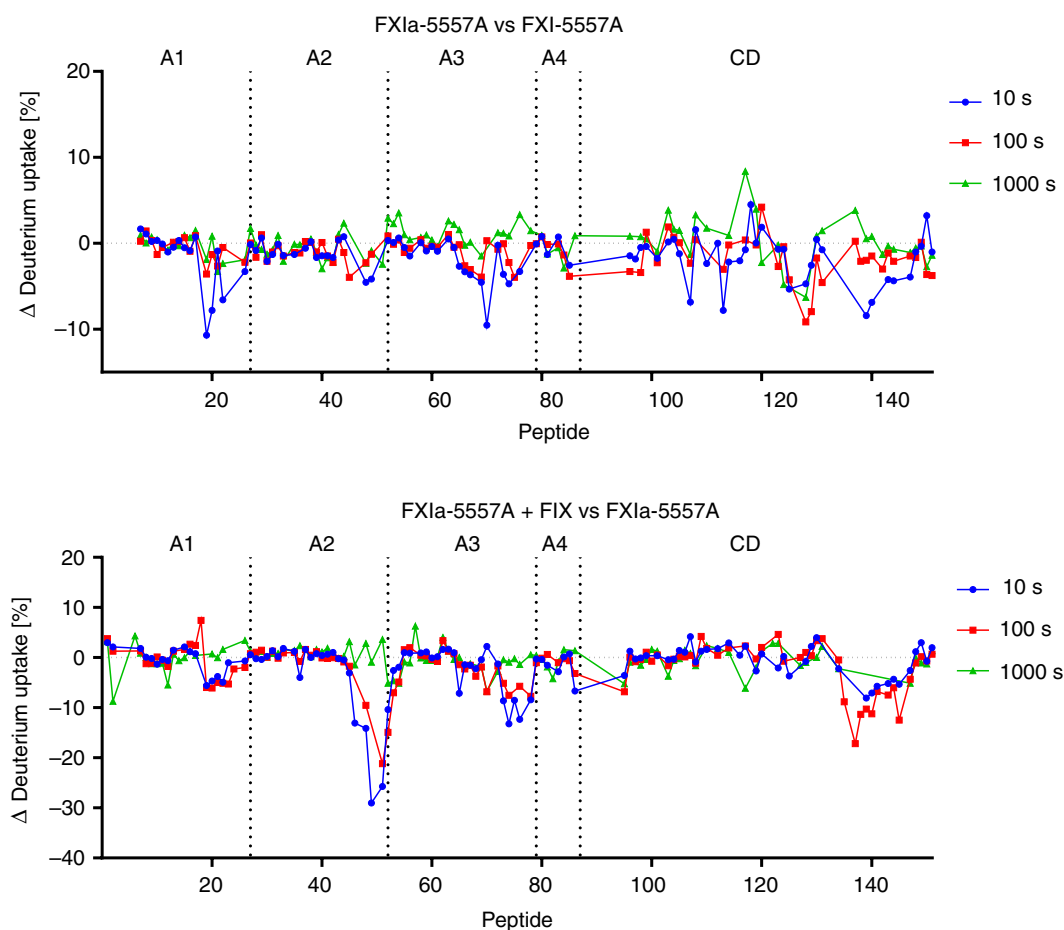


**FIGURE 1** The differences in deuterium uptake ( $\Delta$  Deuterium uptake) plotted for each detected peptide. The deuterium uptake compared between FXI and FXIa (top) is representative of the changes induced by activation. The differences in deuterium uptake between FXIa with FIX and FXIa (bottom) indicate the areas that are affected by binding to FIX

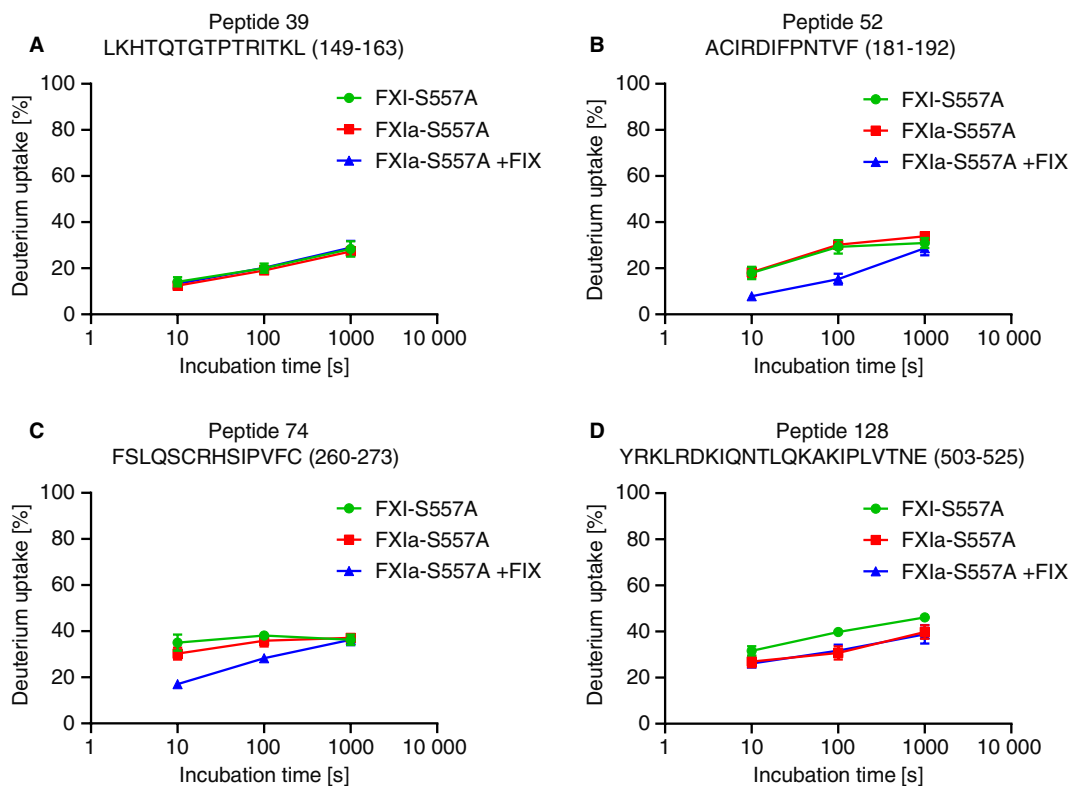


**FIGURE 2** Deuterium uptake graphs of representative peptides. A, Region Leu149-Leu163 (peptide 39) shows an unaltered deuterium uptake between FXI, FXIa, and FXIa with FIX. B, Ala181-Phe192 (peptide 52) shows no difference between FXI and FXIa but deuterium uptake is decreased by the addition of FIX. C, Deuterium uptake of Phe260-Cys273 (peptide 74) is reduced slightly in FXIa and is further decreased for FXIa with FIX. D, Tyr503-Glu525 (peptide 128) undergoes a decrease in deuterium uptake upon activation, but is not influenced by the presence of FIX

loops upon FXI activation, but they are both more accessible and less structured in the FXIa model compared to the FXI crystal structure. The loop contained a helix in the FXI crystal structure, which was not observed in the FXIa model. The accessibility of the beta-strand in apple 3 (Pro<sup>247</sup>-Gly<sup>259</sup>, orange) remains relatively unchanged in the FXIa model, but the region is less structured in the model. Despite the large rotation of the catalytic domain, the regions Lys<sup>509</sup>-Glu<sup>525</sup> (cyan) and Cys<sup>581</sup>-Tyr<sup>590</sup> (yellow) remain structurally unchanged. The accessibility of the Lys<sup>509</sup>-Glu<sup>525</sup> (cyan) appears to be reduced slightly due to a conformational change of the activation loop, defined by the position of Ile<sup>370</sup>, but no changes in accessibility were observed for Cys<sup>581</sup>-Tyr<sup>590</sup>.

### 3.3 | FIX binds to the apple 3 domain in FXIa

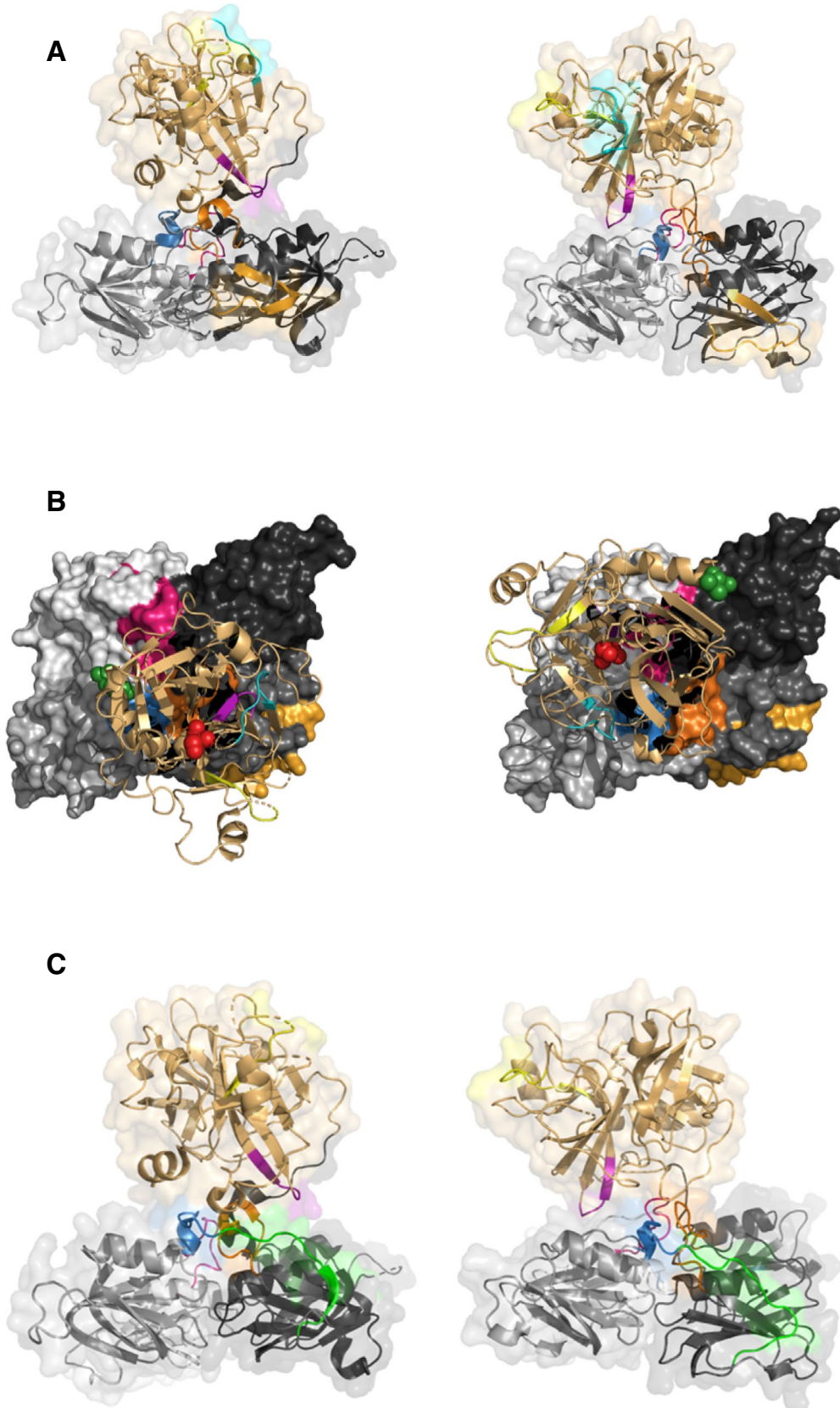
When a difference in deuterium uptake was observed in multiple peptides covering a particular region upon binding of FIX to FXIa we considered this as a change. As seen when highlighted in the FXI crystal structure (Figure 3C, left), these regions greatly correspond to those with an altered deuterium uptake for FXI activation. A small additional reduction in deuterium uptake was observed for the loop between the apple 1 and apple 2 domain (Tyr<sup>80</sup>-Ala<sup>91</sup>, pink) and catalytic region Cys<sup>581</sup>-Tyr<sup>590</sup> (yellow). On the other hand, larger reductions in deuterium uptake were observed for the loop between the

apple 2 and apple 3 domain (Lys<sup>173</sup>-Leu<sup>180</sup>, blue) and the loop between the apple 3 and apple 4 domain (Ser<sup>261</sup>-Phe<sup>272</sup>, dark orange). Moreover, amino acids Ala<sup>181</sup>-Phe<sup>192</sup> (green), which lay adjacent to both regions, showed a large (up to 14.9%) reduction in deuterium uptake, unique to binding of FIX.

Again, these regions were also plotted in the FXIa homology model (Figure 3C, right) and their conformation was compared to that in the FXI crystal structure. Similar to activation, amino acids Cys<sup>581</sup>-Tyr<sup>590</sup> (yellow) showed no structural or accessibility differences. Region Tyr<sup>80</sup>-Ala<sup>91</sup> (pink) was less exposed in the FXIa model compared to the FXI crystal structure as a result from a turn of the catalytic domain. Binding also influenced the loop connecting the apple 2 and apple 3 domains (Lys<sup>173</sup>-Leu<sup>180</sup>, blue) and the loop connecting the apple 3 and apple 4 domains (Ser<sup>261</sup>-Phe<sup>272</sup>, dark orange), which are more exposed in the FXIa model than in the FXI crystal structure. Lastly, the region at the beginning of the apple 3 domain (Ala<sup>181</sup>-Phe<sup>192</sup>, green) appears to be more exposed to the surface in the FXIa model, but shows a greater rigidity in the FXI crystal structure.

## 4 | DISCUSSION

We have performed HDX MS on FXI, FXIa, and FXIa in complex with FIX to identify the areas that undergo molecular changes either upon



activation or by binding to FIX. These affected protein regions were plotted in the crystal structure of FXI and FXIa homology model for both activation (Figure 3A) and binding (Figure 3C).

The affected regions for activation all showed a reduction in the deuterium uptake. This could result from either a reduced accessibility to the solvent or an increased rigidity of these regions in

**FIGURE 3** Regions with an altered deuterium uptake corresponding to activation (A, side view; B, top view) or binding (C) were highlighted in the 3D structure of FXI (left) and in the 3D homology model of FXIa based on the kallikrein crystal structure (PDB ID 6I44)<sup>20</sup> (right). The catalytic domain is coloured beige and the apple domains are coloured lightest (1) to darkest (4). In the top view, the catalytic domain is in ribbon style to better visualize the changes between the structure and model. In panel B, the C-terminus is labelled dark green, and the active site serine in red. Both activation and binding influenced the deuterium uptake for the loops connecting A1, A2, A3, and A4 (coloured pink, blue, and dark orange, respectively) and Cys581-Tyr590 (yellow). Additionally, activation influenced the structure of the apple 3 domain (orange), a loop at the surface of the catalytic domain (cyan), and resulted in movement of the C-terminus of the catalytic domain. FIX binding uniquely affected region Ala181-Phe192 at the beginning of the apple 3 domain (green)

the protein. A small reduction in deuterium uptake was observed for the loop between the apple 2 and the apple 3 domain (Ser<sup>171</sup>-Leu<sup>177</sup>, blue), a beta-strand in the apple 3 domain (Pro<sup>247</sup>-Gly<sup>259</sup>, orange), and the loop between the apple 3 and the apple 4 domain (Ser<sup>281</sup>-Phe<sup>272</sup>, dark orange). Whereas this could be assigned to a reduced accessibility for Pro<sup>247</sup>-Gly<sup>259</sup> (orange), this contradicts the

increased exposure of regions Ser<sup>171</sup>-Leu<sup>177</sup> (blue) and Ser<sup>281</sup>-Phe<sup>272</sup> (dark orange) resulting from a 180° turn of the catalytic domain in the FXIa model. Especially, the loop between the apple 3 and apple 4 has already been shown to go from a buried conformation in the inactive zymogen to being exposed on the protein surface in active kallikrein.<sup>20</sup>

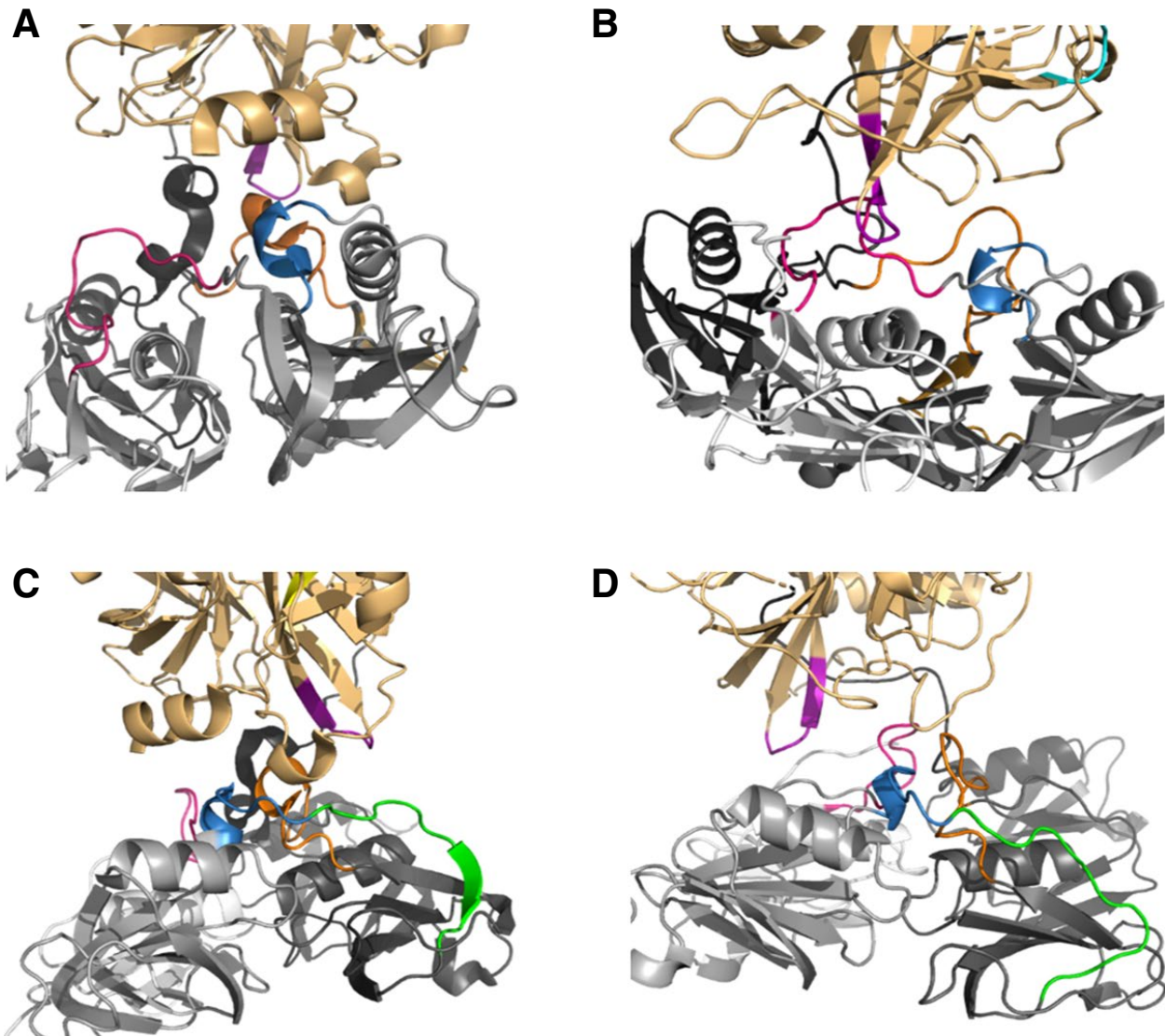


**FIGURE 4** Regions with an altered deuterium uptake corresponding to activation (A and B) or binding (C and D) were highlighted in the 3D structure of FXI (left) and in the 3D homology model of FXIa based on the kallikrein crystal structure<sup>20</sup> (right). The catalytic domain is coloured beige and the apple domains are coloured lightest (1) to darkest (4). Residues Asn566-His570 are coloured purple. Activation clearly decreased the accessibility of the loop connecting the apple 1 and apple 2 domains (pink). On the other hand, the loop between the apple 2 and 3 domains (blue) and the loop between the apple 3 and apple 4 domains (dark orange), and Ala181-Phe192 showed increased accessibility upon activation and were further affected by binding of FIX

Although we cannot exclude the possibility that the lower deuterium uptake is due to reduced exposure of the apple 3 domain, we propose that the discrepancy between the greater accessibility in the FXIa model and the observed decrease in deuterium exchange is the result of an increased rigidity of the protein region in FXIa. Thus, the higher rigidity would compensate for the gain in hydrogen deuterium exchange from an increased accessibility of the loop. We also propose that the helix seen in the FXI crystal structure is not observed in the FXIa model because it is based on the structure of kallikrein, for which HDX MS did not indicate such increased rigidity.<sup>20</sup> This difference could explain ligand selectivity, with FIX binding to FXIa but not to kallikrein. Furthermore, this supports the general hypothesis that the loop between the apple 3 and apple 4 domains in FXI mediates substrate binding.<sup>13,14</sup>

Interestingly, a stronger reduction in deuterium uptake was observed for the loop connecting the apple 1 and apple 2 domain (Tyr<sup>80</sup>-Ala<sup>91</sup>, pink), which supports the turn of the catalytic domain. This region is very exposed to the surface in the FXI crystal structure and becomes much more shielded in the FXIa model, where it is buried within the interface between the catalytic domain and the apple domains. The difference in accessibility of this region in FXI and the FXIa model is highlighted in Figure 4A,B, respectively.

In the catalytic domain molecular changes were observed for regions Lys<sup>509</sup>-Glu<sup>525</sup> (cyan) and Cys<sup>581</sup>-Tyr<sup>590</sup> (yellow). For both areas a lower deuterium uptake was observed in FXIa compared to FXI. For Lys<sup>509</sup>-Glu<sup>525</sup>, located at the surface of the catalytic domain, this may be caused by a reduced accessibility as a result from movement of the activation loop upon activation. This corresponds to results obtained in a previous study using tandem mass tag mass spectrometry that suggested shielding of the region by the released activation loop after cleavage.<sup>23</sup>

On the other hand, the accessibility of region Cys<sup>581</sup>-Tyr<sup>590</sup> does not appear to be affected by activation when comparing the 3D protein structures. Thus, the difference in deuterium uptake could be explained by an increase in rigidity. This might be caused by the direct connection to residues Asn<sup>566</sup>-His<sup>570</sup> (Figure 3A, purple), which form a loop that serves as an important latch between the catalytic domain and the apple domains after the activation loop is cleaved. The latch has been shown to move 40 Å in kallikrein to form new interactions with the apple domains.<sup>20</sup> This movement could increase the strain in Cys<sup>581</sup>-Tyr<sup>590</sup>, resulting in a lower uptake of deuterium. Moreover, the changed interaction site of the latch loop is likely related to the turn of the catalytic domain.

#### 4.1 | Molecular changes induced by FIX binding to FXIa

The majority of the regions affected by binding to FIX were also affected by activation, suggesting that the protein undergoes these molecular changes to accommodate FIX binding. Binding of

FIX induced small molecular changes in FXIa for residues Tyr<sup>80</sup>-Ala<sup>91</sup> (pink) and Cys<sup>581</sup>-Tyr<sup>590</sup> (yellow). This could be an indication that these regions are mainly affected by the structural changes required to allow FIX binding but do not interact directly with the substrate.

Larger differences were seen for the loops connecting the apple 2 and apple 3 domain (Lys<sup>173</sup>-Leu<sup>180</sup>, blue) and the apple 3 and apple 4 domain (Ser<sup>261</sup>-Phe<sup>272</sup>). Furthermore, residues Ala<sup>181</sup>-Phe<sup>192</sup> (green) at the beginning of the apple 3 domain were uniquely influenced by binding of FIX. Interestingly, this region in the apple 3 domain includes the amino acids Ile<sup>183</sup>, Arg<sup>184</sup>, and Asp<sup>185</sup>, which in point mutation studies have shown to be involved in FIX binding.<sup>15</sup> Since the two loops are in close proximity to the proposed binding site, the reduction in deuterium uptake could be caused either by direct interactions with FIX or by shielding of these regions by FIX after binding to residues Ala<sup>181</sup>-Phe<sup>192</sup>.

Interestingly, regions Lys<sup>173</sup>-Leu<sup>180</sup> (blue), Ser<sup>261</sup>-Phe<sup>272</sup> (dark orange), and Ala<sup>181</sup>-Phe<sup>192</sup> (green) are less structured in the FXIa model (Figure 4D) compared to the FXI crystal structure (Figure 4C), whereas HDX MS suggests that their rigidity has increased. This discrepancy might be because the FXIa model is based on the crystal structure of kallikrein (PDB ID 6I44),<sup>20</sup> which does not bind to FIX. Thus, the increased rigidity of the loops between the apple 2 and apple 3 domain and between the apple 3 and 4 domain during activation could be necessary to mediate FIX binding to the proposed binding site in the apple 3 domain. The fact that these regions show great flexibility in the kallikrein crystal structure could be the basis for the difference in substrate selectivity between kallikrein and FXIa.

In conclusion, based on the prekallikrein model it was proposed that upon activation the catalytic domain turns a 180° with respect to the plane of apple domains.<sup>20</sup> Our HDX MS data suggest a similar activation mechanism for FXI with a turn of the catalytic domain uncovering the apple 3 domain to allow binding of FIX. Furthermore, our results confirm the proposed FIX binding region (Ala<sup>181</sup>-Phe<sup>192</sup>) and highlight the influence of binding on the loops between the apple 2 and apple 3 domain and between the apple 3 and apple 4 domain. These loops are in close proximity to the FIX binding region and might also mediate FIX binding, which could be linked to their increased rigidity after FXI activation. Surprisingly, this increased rigidity was not observed in the FXIa model, which may be the result of using kallikrein as the scaffold for the FXIa model. Kallikrein does not bind FIX and a difference in rigidity of these regions in FXIa could be the basis for the different binding profiles of the two proteins. These proposed molecular changes should be verified by the elucidation of the crystal structure of FXIa and the FXIa-FIX complex.

#### ACKNOWLEDGEMENTS

This research was supported by grant PPOP-14-01 (Netherlands Ministry of Health), and grant 1702 from the Landsteiner Foundation for Blood Research.



## CONFLICT OF INTEREST

The employer of JCMM (Sanquin) received honoraria for participation in scientific advisory board panels and consulting for Bayer and Daiichi Sankyo. The other authors have no conflict of interest.

## AUTHOR CONTRIBUTIONS

JCMM and ABM designed and supervised the study. ABB, JvG, IS, JAM performed experiments and analysed data. All authors were involved in interpretation of the data. ABB wrote the manuscript with input from all authors. All authors approved the final manuscript.

## ORCID

Awital Bar Barroeta  <https://orcid.org/0000-0002-0744-5569>

Alexander B. Meijer  <https://orcid.org/0000-0002-5447-7838>

Joost C. M. Meijers  <https://orcid.org/0000-0002-4198-6780>

## LINKED CONTENT

See also Gailani, D., Emsley, J. Toward a better understanding of factor XI activation. *J Thromb Haemost.* 2019;17:2016–2018. <https://doi.org/10.1111/jth.14631>

## REFERENCES

1. Emsley J, McEwan PA, Gailani D. Structure and function of factor XI. *Blood.* 2010;115:2569–2577.
2. Mohammed B, Matafonov A, Ivanov I, et al. An update on FXI structure and function. *Thromb Res.* 2018;161:94–105.
3. Von dem Borne PAK, Bajzar L, Meijers JCM, Nesheim ME, Bouma BN. Thrombin-mediated activation of factor XI results in a thrombin-activatable fibrinolysis inhibitor-dependent inhibition of fibrinolysis. *J Clin Invest.* 1997;99:2323–2327.
4. Von dem Borne PAK, Meijers JCM, Bouma BN. Feedback activation of factor XI by thrombin in plasma results in additional formation of thrombin that protects fibrin clots from fibrinolysis. *Blood.* 1995;86:3035–3042.
5. James P, Salomon O, Mikovic D, Peyvandi F. Rare bleeding disorders - bleeding assessment tools, laboratory aspects and phenotype and therapy of FXI deficiency. *Haemophilia.* 2014;20:71–75.
6. Meijers JCM, Tekelenburg WLH, Bouma BN, Bertina RM, Rosendaal FR. High levels of coagulation factor XI as a risk factor for venous thrombosis. *N Engl J Med.* 2000;342:696–701.
7. Yang DT, Flanders MM, Kim H, Rodgers GM. Elevated factor XI activity levels are associated with an increased odds ratio for cerebrovascular events. *Am J Clin Pathol.* 2006;126:411–415.
8. Löwenberg EC, Meijers JCM, Monia BP, Levi M. Coagulation factor XI as a novel target for antithrombotic treatment. *J Thromb Haemost.* 2010;8:2349–2357.
9. Doggen CJM, Rosendaal FR, Meijers JCM. Levels of intrinsic coagulation factors and the risk of myocardial infarction among men: opposite and synergistic effects of factors XI and XII. *Blood.* 2006;108:4045–4051.

10. Papagrigroriou E, McEwan PA, Walsh PN, Emsley J. Crystal structure of the factor XI zymogen reveals a pathway for transactivation. *Nat Struct Mol Biol.* 2006;13:557–558.
11. Geng Y, Verhamme IM, Smith SB, et al. The dimeric structure of factor XI and zymogen activation. *Blood.* 2013;121:3962–3969.
12. Navaneetham D, Jin L, Pandey P, et al. Structural and mutational analysis of the molecular interactions between the catalytic domain of factor XIa and the Kunitz protease inhibitor domain of protease nexin 2. *J Biol Chem.* 2005;280:36165–36175.
13. Gailani D, Geng Y, Verhamme I, et al. The mechanism underlying activation of factor IX by factor XIa. *Thromb Res.* 2014;133:S48–S51.
14. Smith SB, Verhamme IM, Sun M, Bock PE, Gailani D. Characterization of novel forms of coagulation factor XIa. *J Biol Chem.* 2008;283:6696–6705.
15. Geng Y, Verhamme IM, Sun MF, Bajaj SP, Emsley J, Gailani D. Analysis of the factor XI variant Arg184Gly suggests a structural basis for factor IX binding to factor XIa. *J Thromb Haemost.* 2013;11:1374–1384.
16. Geng Y, Verhamme IM, Messer A, et al. A sequential mechanism for exosite-mediated factor IX activation by factor XIa. *J Biol Chem.* 2012;287:38200–38209.
17. Sun YH, Gailani D. Identification of a factor IX binding site on the third apple domain of activated factor XI. *J Biol Chem.* 1996;271:29023–29028.
18. Sun MF, Zhao M, Gailani D. Identification of amino acids in the factor XI apple 3 domain required for activation of factor IX. *J Biol Chem.* 1999;274:36373–36378.
19. McMullen B, Fujikawa K, Davie E. Location of the disulfide bonds in human coagulation factor XI: the presence of tandem apple domains. *Biochemistry.* 1991;30:2056–2060.
20. Li C, Voos KM, Pathak M, et al. Plasma kallikrein structure reveals apple domain disc rotated conformation compared to factor XI. *J Thromb Haemost.* 2019;17:759–770.
21. Konermann L, Pan J, Liu YH. Hydrogen exchange mass spectrometry for studying protein structure and dynamics. *Chem Soc Rev.* 2011;40:1224–1234.
22. Naito K, Fujikawa K. Activation of human blood coagulation factor xi independent of factor XII. *J Biol Chem.* 1991;266:7353–7358.
23. Stroo I, Marquart JA, Meijers JCM, Bakhtiari K, Meijer AB. Chemical footprinting reveals conformational changes following activation of factor XI. *Thromb Haemost.* 2018;118:340–350.

## SUPPORTING INFORMATION

Additional supporting information may be found online in the Supporting Information section at the end of the article.

**How to cite this article:** Bar Barroeta A, van Galen J, Stroo I, Marquart JA, Meijer AB, Meijers JCM. Hydrogen-deuterium exchange mass spectrometry highlights conformational changes induced by factor XI activation and binding of factor IX to factor XIa. *J Thromb Haemost.* 2019;17:2047–2055. <https://doi.org/10.1111/jth.14632>